IEEE Access
Multidisciplinary | Rapid Review | Open Access Journal

Received 22 May 2022, accepted 15 July 2022, date of publication 19 July 2022, date of current version 22 July 2022.

Digital Object Identifier 10.1109/ACCESS.2022.3192425

RESEARCH ARTICLE

High-Precision Static Alignment Scheme Based on the Eigenfrequency Separation Characteristics of Same-Order Hermite-Gaussian Mode in Triangular Ring-Down Cavities

YIJIE REN[1,2], CHANGXIANG YAN[1,3], CONGJUN WU[1], XIAOQUAN BAI[1,2], AND ZHIWEI CHEN[1,2]

[1]Changchun Institute of Optics, Fine Mechanics and Physics, Chinese Academy of Sciences, Changchun 130033, China
[2]College of Materials Science and Opto-Electronic Technology, University of Chinese Academy of Sciences, Beijing 100049, China
[3]Center of Materials Science and Optoelectrics Engineering, University of Chinese Academy of Science, Beijing 100049, China

Corresponding author: Congjun Wu (wucongjun789@163.com)

This work was supported in part by the National Natural Science Foundation of China (NSFC) under Grant 61805235, Grant 61905241, and Grant 61875192.

ABSTRACT Triangular cavities are increasingly used in cavity ring-down spectrometers (CRDS) to compensate for the existence of optical feedback and other disadvantages of straight cavities. However, at the same time, the difficulty of the cavity mounting alignment process is increased. Consequently, the fast and stable establishment of resonance between the optical source and the triangular ring-down cavity has been widely explored for CRDS-based applications. The Hermite-Gaussian theory has unique advantages for the description of the Gaussian resonant beams characteristics in triangular cavities, while the theory is of great importance for the alignment in high finesse triangular ring-down cavities. Along these lines, in this work, the eigenfrequency separation characteristics of the Hermite-Gaussian modes in the triangular cavity, in the meridional and sagittal planes, as well as the excitation and transmission characteristics of the first-order mode in the high finesse cavity were verified. A static alignment method was established for the high-finesse triangular ring-down cavity, and the transmission suppression of the Hermite-Gaussian modes by the high-finesse cavity was overcome in the experiment. Finally, by leveraging the advantageous features of the fundamental and the first-order mode that are complementary to each other, the tilt and axis shift errors of each specified plane with directional high accuracy can be aligned. The static alignment scheme of the triangular cavity based on the Hermite-Gaussian theory that was established here paves the way for the mounting alignment of the CRDS instrument before the ring-down experiment, whereas the system accuracy of CRDS is further improved.

INDEX TERMS CRDS, Hermite-Gaussian mode, misalignment, triangular cavity.

I. INTRODUCTION

In recent years, the cavity ring-down spectroscopy (CRDS) technique has been used extensively in the field of trace gas detection in complex environments due to its advantages, in terms of detection speed and accuracy. It has been also used to measure the concentration of trace gases in-ground, space and deep sea for environmental protection, resource detection, etc. [1]–[6]. CRDS has been also recently employed in fields such as biomedicine for the prevention and diagnosis of several diseases, which has further broadened its potential application [7], [8]. It also has powerful advantages in terms of detection of nuclear particles and explosives, etc. [9]–[11]. Recently, CRDS has been implemented in the fields of Boltzmann constant determination by optical thermometry and isotope ratio measurement [12], [13], which requires a higher accuracy from the instrument.

In order to improve the accuracy and stability of the instrument, the CRDS has undergone a series of structural developments, especially the core structures such as the light

The associate editor coordinating the review of this manuscript and approving it for publication was Chao Zuo.

source and the ring-down cavity (CDR). The light source undergoes the transformation from the pulsed light source to the continuous-wave laser. The CDR as a critical structure induced the improvement from straight to triangular cavity. The triangular cavity improves the optical feedback of the straight cavity and the standard tool effect [14], which further enhances the frequency stability of the light source. Nevertheless, the difficulty of the system installation and adjustment is increased.

Interestingly, achieving stable resonance between the light source and the resonant cavity is regarded as a key technology for CRDS-based instruments. Most of the existing solution ideas rely on the improvement of dynamic frequency stabilization [15], [16]. The PDH method has become a common approach among the existing dynamic frequency stabilization techniques [17], [18]. More specifically, the PDH method is a dynamic adjustment method to maintain stable CDR resonance during the measurement. However, the existence of a relatively high precision mounting alignment is a prerequisite for achieving the resonance effect. The high-finesse cavity also suppresses the transmission of the HGS modes (HGS modes refer to modes other than the fundamental mode), which makes alignment more difficult. The precise alignment between each cavity mirror and the laser source prior to the ring-down experiment is called the static alignment technique.

The analysis based on the Hermite-Gaussian (HGS) theory is widely used in the field of gravitational-wave mode cleaners and other fields during the static mounting alignment phase. Several mature applications of the HGS theory in the field of straight cavities and four-mirror cavities have been reported in the literature [19]–[22]. As far as the theoretical study of the HGS of triangular cavities is concerned, the misalignment of triangular cavities with different structures has been studied by Song [23], whereas a systematic summary of the frequency, mode, and polarization characteristics of the triangular cavity has been presented by Saraf [24]. However, the high-precision static alignment technique of triangular cavities based on HGS modes has not been investigated.

As the demands for CRDS precision metrics are constantly increased, higher finesse cavities are used to enhance the effective absorbed light range in the cavity. The higher reflectivity increases the time constant of the cavity, thus enabling an improved theoretical detection accuracy of the instrument [25]–[27]. However, this technique also leads to a decrease in the cavity throughput, and the optical energy of the system is reduced. As a result, the detector's noise is regarded as the primary factor that limits sensitivity and limits the manifestation of a high accuracy static alignment [28].

We have to underline that the existing PDH methods can achieve dynamic stabilization of the cavity resonance. However, high-precision static alignment of the cavity mirror with the light source is required before the dynamic stabilization process to achieve high-precision trace gas concentration measurements. No such complete static alignment scheme has been proposed yet. Although static alignment schemes based on HGS theory have been investigated in straight cavities and four-mirror annular cavities, the triangular cavity needs to be subjected to a more complicated alignment process due to its more complex structure than the straight cavity. In addition, the use of high finesse cavities reduces the optical energy of the system. Therefore, the proposed static alignment scheme of high finesse triangular CDR is considered quite significant for CRDS to achieve theoretical sensitivity.

Under this direction, in this work, the sources of mounting difficulties in CRDS based on high-finesse triangular CDR and the final solutions were systematically analyzed. Then, a high-precision static alignment method based on the first-order HGS mode was proposed based on the unique HGS mode frequency separation characteristics of the triangular cavity. The transmission suppression of the HGS mode by a high-finesse cavity was refined in the experimental scheme. Finally, a perfect scheme combining both the fundamental mode monotonicity and the first-order mode split-plane alignment property was developed. Interestingly, the split-plane directional alignment of the triangular cavity system has been realized for the first time. The alignment efficiency and accuracy during the process of CRDS high finesse ring-down cavity mounting is not only improved but also the resonance theory system of the high finesse triangular cavity is validated.

The goal of this work is to elaborate on the theoretical system and implementation scheme of the high-precision static alignment scheme. In Section 2, the limitation of sensitivity by the high finesse triangular CDR is firstly analyzed. Subsequently, the frequency separation characteristics of the same order HGS mode unique to the triple resonant cavity are explored, as well as the excitation and transmission characteristics of the first-order mode are derived. In Section 3, experiments are established based on the frequency separation characteristics of the HGS mode in the meridional and sagittal planes to verify the excitation relation of the maladjustment to the first-order mode. Since the first-order mode exhibits non-monotonicity as the misalignment error is increased, Section 4 establishes a refined static alignment scheme based on the original scheme by combining the monotonicity of the fundamental mode to overcome the drawbacks of the first-order mode. The conclusions are given in Section 5.

II. HERMITE-GAUSSIAN MODE EXCITATION AND TRANSMISSION CHARACTERISTICS OF A HIGH FINESSE TRIANGULAR CDR CAVITY

The CRDS system based on a triangular CDR uses the same triangular ring resonant cavity as the gravitational wave detection mode cleaner and the laser gyroscope systems. However, the transmission energy of the system is suppressed due to the extremely high cavity reflectivity and narrow source linewidth of CRDS. The first part of this chapter systematically analyzes the underlying origins of energy loss in the high-finesse triangular CDR and derives the sensitivity expressions for this system. In the second part, the theoretical

root of this work is introduced, and the various excitation properties of first-order HGS mode. The frequency separation characteristics of the first-order mode in the triangular cavity and the transmission characteristics of the first-order mode in the high-finesse cavity are also analyzed.

A. SENSITIVITY ANALYSIS OF HIGH FINESSE TRIANGULAR CAVITY CRDS SYSTEM

The time constant is regarded as an important measure of the CRDS system and it depends on the reflectivity of the cavity. The ring-down time τ_0 of the cavity is given by equation (1) [29], where τ_0 represents the time taken for the light intensity to ring-down to e^{-1} of the initial intensity.

$$\tau_0 = \frac{l}{c(1-R)} \tag{1}$$

where l is the length of the passive cavity, c stands for the speed of light, and R denotes the reflectivity of the cavity mirror. In order to increase the time constant of the CDR, the cavity reflectivity of the CDR was generally considered 99.9% or more, whereas to achieve the measurement accuracy at the *ppb* (part per billion) level, the reflectivity of some cavities even reached the value of 99.997% [23].

Without considering the loss of other factors, the final transmitted light intensity of the triangular cavity can be expressed as follows (2):

$$I^0_{\text{trans}} = I_0 \frac{T_1 T_2}{1 + R_1 R_2 R_3 - 2\sqrt{R_1 R_2 R_3}\cos\varphi} \tag{2}$$

where $R_1R_2R_3$ and $T_1T_2T_3$ are the reflectance and transmittance of $P_1P_2P_3$, respectively, and φ denotes the phase difference of light in one round trip in the cavity. When resonance is reached, $\cos\varphi = 1$.

The final transmitted light intensity of a triangular cavity is also influenced by multiple factors. Firstly, the loss due to the linewidth of the light source and the cavity linewidth was analyzed, while the loss due to the linewidth difference between them is called linewidth ratio loss. The linewidth of a high finesse cavity can be expressed as follows (3):

$$\Delta\omega_{fwhm} = \frac{FSR}{F} \tag{3}$$

where FSR is the free spectral range of the cavity and F is the finesse of the cavity, which is determined by the cavity mirror reflectance. The linewidth ratio loss is also denoted by χ. From (4), it can be concluded that the increase of the cavity's reflectivity leads to an elevated linewidth ratio loss.

$$\chi = \frac{\Delta\nu_{in} F}{FSR} \tag{4}$$

where $\Delta\nu_{in}$ is the line width of the light source.

During the actual detection, in addition to the line-to-width ratio loss, cavity surface absorption and scattering losses, beam line shape mismatch loss, mode mismatch loss and other factors take also place. The complete expression of the final light energy emitted from the triangular cavity is calculated as follows (5):

$$E_{\text{trans}} = \sqrt{T_1 T_2} e^{-i\varphi} \sum_{n=1}^{\infty} \left[\sqrt{R_1 R_2 R_3} e^{-i\varphi}\right]^{n-1} \cdot \sqrt{\chi \cdot S \cdot U \cdot V} E_{in} \tag{5}$$

where S is the loss coefficient of absorption and scattering from the cavity surface, which is determined by the cavity mirror, and U denotes the mismatch coefficient between the light source and the beam line shape in the cavity, which depends on the beam shaping effect of the matching mirror, and V represents the fundamental mode loss coefficient that can be expressed from equation (6). The currently known causative factor is the increase of the mode volume due to the misalignment mismatch.

$$V = \frac{P_{00}}{\sum_{m=0,n=0}^{m\infty,n=\infty} P_{mn}} \tag{6}$$

where P_{00} represents the power of the base mode and P_{mn} is the power of the other HGS modes.

The sensitivity of a CRDS system in the ideal case is generally expressed by equation (7), which is the ratio of the loss of light in one round trip ΔI in the cavity to the most intense light intensity I_{Cmax} established in the cavity. Although this method describes sensitivity, it is applicable to common situations. However, the sensitivity limit for the case where detector noise dominates has not been widely known until recently [14].

$$\delta I = \frac{\Delta I}{I_{C\max}} \tag{7}$$

where ΔI is determined by k.

$$\kappa = (1 - T_1 - T_2 - T_3 - S - \alpha L) \tag{8}$$

As the cavity reflectivity increases, the suppression of the transmitted energy by the high-finesse cavity reaches the order of 10^{-8} or even higher, as is shown by equation (5). When δI is less than the minimum detection limit of the detector, the actual sensitivity is limited by the detector itself regardless of the single round-trip loss of the CDR. Therefore, the sensitivity of the triangular cavity is limited by both the time and the intensity responses.

On top of that, when the finesse of the system is low, the light range energy loss for one week is large. Since the time response is the main factor limiting the sensitivity, the sensitivity can be expressed by equation (7). Under this perspective, as the finesse of the resonant cavity becomes larger, the light energy loss per cycle is well below the detection limit of the detector. In the case the sensitivity is affected by the intensity response, it can be expressed by equation (9) [14]:

$$\sigma_\alpha = \frac{\sqrt{2}\sigma_{\ln\tau}}{l_{eff} N_p} \tag{9}$$

where $\sigma_{ln\tau}$ is the ratio of experimental RMS noise in the ring-down [30], which mainly includes noise introduced by the detection electrons (amplifier noise, thermal noise circuit resistance, or detector dark current), noise generated by the data acquisition system (digital oscilloscope quantization), and noise generated by changes in experimental conditions (cavity path length variation or laser-cavity mode coupling). In addition, l_{eff} is the effective path length, N_p represents the number of photons reaching the detector. Obviously by increasing l_{eff}, N_p is decreased, and increasing N_p while maintaining the effective path length constant is considered an important tool. Consequently, if the reflectivity of the cavity mirror is reasonably designed with the same cavity finesse, the sensitivity of the instrument can be improved.

The transmission coefficient of the triangular CDR can be expressed as k_T, whereas as can be seen from Eq. (11), both R_1 and R_2 have the same impact on the final transmission coefficient. Obviously, R_1, R_2, and R_3 have also the same impact on the finesse of the cavity, but the increase of R_3 has a weaker suppression of the transmission coefficient than the input and output mirrors. This effect allows the use of an increased end-mirror reflectivity to ensure cavity refinement, while R_1 and R_2 can be reduced. Thereby, the limitations in detector intensity response are decreased. The above-mentioned analysis provides the basis for the choice of the cavity mirror in the experiment. The conclusion is also in striking agreement with the impedance matching theory of the triangular resonant cavity. Full power injection can be achieved by placing T_1, and T_2 above T_3 by roughly 10^2 magnitudes.

$$k_T = \frac{(1-R_1)(1-R_2)}{1+R_1R_2R_3-2\sqrt{R_1R_2R_3}\frac{\pi\sqrt[6]{R_1R_2R_3}}{1-\sqrt[3]{R_1R_2R_3}}} \tag{10}$$

B. FREQUENCY SEPARATION CHARACTERISTICS OF TRIANGULAR CAVITY FIRST-ORDER HGS MODE

In many reports in the literature where resonant cavities have been examined, an appropriate combination of geometrical optics and diffraction theory has been used as a classical theory. More specifically, Hermite-Gaussian functions are increasingly used for the expression of lasers. The q-parameter of a Gaussian beam in a resonant cavity can be expressed as follows: $\frac{1}{q} = \frac{1}{\rho} - i\frac{\lambda}{\pi\omega^2}$ by using its wavefront curvature ρ and beam waist size ω. The beam waist ω can be expressed as follows (11):

$$\omega_0^2 = \left|\frac{\lambda}{2\pi C}\sqrt{4-(A+D)^2}\right|. \tag{11}$$

When the cavity structure meets the stability condition, $|A+D|<2$, the propagation of the Gaussian beam q parameter can be equated to the propagation equation $q_2 = \frac{Aq_1+B}{Cq_1+D}$ of an ordinary spherical wave. The $ABCD$ parameter can be expressed as follows (13) [31]:

$$M = \begin{vmatrix} A & B \\ C & D \end{vmatrix} = \begin{vmatrix} 1-\frac{2(L_1+L_2)}{R} & L_1+L_2+L_3-\frac{2L_3(L_1+L_2)}{R} \\ -\frac{2}{R} & 1-\frac{2L_3}{R} \end{vmatrix}. \tag{12}$$

During the actual CRDS setup, the matching of the external laser beam to the cavity mode determines the accuracy of the instrument. As a result, the fundamental mode coupling is only achieved when the light source is perfectly aligned and matched to the cavity mode. Any deviation from this condition will result in an increase in the mode volume. Any misalignment of the passive cavity and the light source in the CRDS system also reduces the energy of the outgoing fundamental mode Gaussian beam and leads to an increase in the ring-down curve fitting error. The limitation of the HGS modes (other than the fundamental mode) has been an important factor to improve the accuracy of the instrument.

The unique HGS mode separation property of the triangular cavity provides the necessary theoretical basis for solving the triangular cavity alignment problem [24]. The separation characteristics of the HGS mode can be explained as follows: the triangular ring cavity with a spherical reflector has different resonant frequencies for the same order modes in two orthogonal planes due to astigmatism. For example, the TEM_{10} in the meridional plane and the TEM_{01} in the sagittal plane in the triangular cavity have different eigenfrequencies, which is the essential difference between the triangular cavity and the straight cavity.

Unlike the polarization theory in which the resonant frequencies of s-light and p-light are different, the eigenfrequency separation of the triangular cavity, where the same order HGS mode in two orthogonal planes exists, can be explained by the Gouy phase [32]. The frequency interval between each order mode of the triangular cavity and the light source can be estimated by equation (13). By assuming that the PDH can stabilize the cavity mode frequency at the center frequency of the light source, $\Delta\nu_{mn}$ denotes the frequency interval between the HGS mode and the fundamental mode.

$$\Delta\nu_{mn} = \frac{FSR}{\pi}(m+n)\arccos\left(\sqrt{1-\frac{L}{R}}\right) + \frac{FSR}{2}\frac{(1-(-1)^m)}{2}. \tag{13}$$

Thus, the eigenfrequencies of TEM_{10} and TEM_{01} are $\Delta\nu_{10}$ and $\Delta\nu_{01}$, respectively, with an interval of $FSR/2$.

$$\Delta\nu_{10} = \frac{FSR}{\pi}\arccos\left(\sqrt{1-\frac{L}{R}}\right)+\frac{FSR}{2}$$
$$\Delta\nu_{01} = \frac{FSR}{\pi}\arccos\left(\sqrt{1-\frac{L}{R}}\right) \tag{14}$$

Since Sayeh proposed the parameters for the misalignment mismatch in a resonant cavity [22], the relationship between the excitation of the first-order mode in a triangular cavity and the misalignment mismatch has been discussed in detail [23]. When only the mismatch exists, the excitation of the first-order mode can be expressed as follows (15):

$$A_1/A_0 = \left(2\pi e^{-2}\right)^{-1/4}(\varepsilon_v - q_{Lv}\alpha_v)\,\omega_0 \tag{15}$$

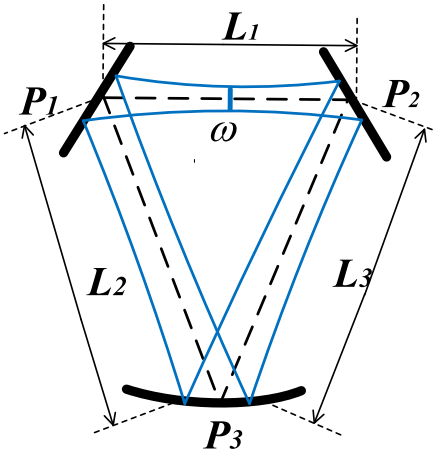

FIGURE 1. Triangular CDR optical path diagram.

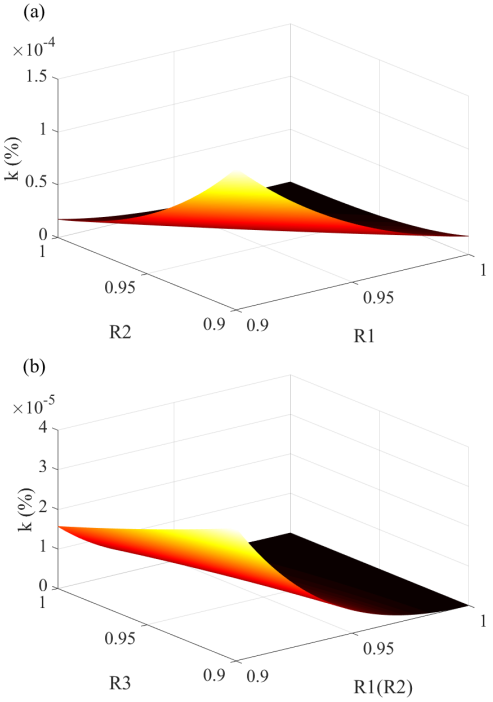

FIGURE 2. Variation of the transmission coefficient of a triangular ring-down cavity with reflectivity of cavity mirrors.

where ε_v is the transverse shift of the optical axis between the injected beam and the intracavity beam, and α_v stands for the tilt of the optical axis between the injected beam and the intracavity beam. Due to the orthogonality of the HGS mode [33], ε_v and α_v in the meridian plane (x-z plane) were analyzed as an example, and the y-z plane can be equated with it. Moreover, q_{Lv} and ω_0 are the q-parameters and beam waist of the intracavity beam. The relationship between excitation and misalignment error of the first-order mode under each triangular cavity structure is depicted in Fig. 3.

By comparing Fig. 2ac with bd, it can be argued that the excitation of the first-order mode caused by the axis tilt is larger than the axis transverse shift. The excitation of the first-order mode by the misalignment shows a tendency to increase and then decrease with the error. When the error is

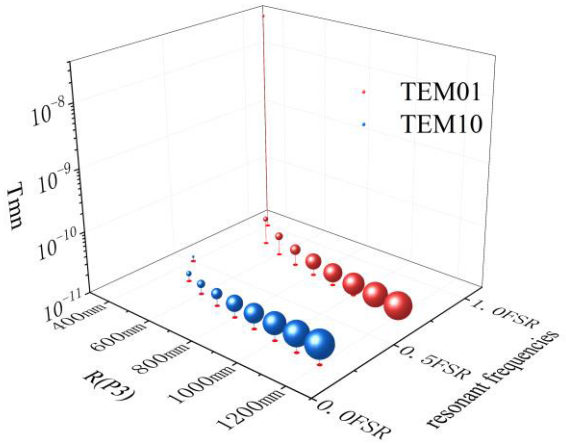

FIGURE 3. Eigenfrequency distribution and transmission intensity of the first-order mode in the meridional and sagittal planes. The radius of the sphere represents the radius of curvature of the end-mirror for different cavity structures.

gradually increased, the excitation of the first-order mode is enhanced. However, when the error is increased to a certain degree, the energy of the first-order mode is also lost sharply as the energy of the system is decreased. The angle a between P_1 and P_2 will not affect the misalignment sensitivity, and the cavity will be more sensitive to the misalignment error when the radius of curvature of P_3 is increased.

The conditions analyzed above include the perfect transmission, while the transmission suppression of the resonant cavity is not considered. The high reflectivity mirror in the high-finesse triangular cavity exhibits a stronger suppression of the transmission of the HGS mode than that of the fundamental mode. The transmission intensity of the first-order mode in the high-finesse cavity can be expressed by equation (16), from which it can be observed the transmission intensity of TEM_{10} and TEM_{01} is proportional to F^2. Therefore, achieving stable detection of first-order mode in high-finesse cavities is the key to first-order mode-guided mounting alignment. Overcoming the suppression of the first-order mode by high finesse cavities in a high-precision static alignment scheme is regarded of vital importance for enhanced transmission intensity.

$$\frac{I_{10}}{I_{00}} = \frac{\left(2\pi e^{-2}\right)^{-1/2} \left(\varepsilon_v - q_{Lv}\alpha_v\right)^2 {\omega_0}^2}{\left[1 + \frac{4F^2}{\pi^2} \sin^2\left(\arccos\left(\sqrt{1 - \frac{L}{R}}\right) + \frac{\pi}{2}\right)\right]^{1/2}},$$
$$\frac{I_{01}}{I_{00}} = \frac{\left(2\pi e^{-2}\right)^{-1/2} \left(\varepsilon_v - q_{Lv}\alpha_v\right)^2 {\omega_0}^2}{\left[1 + \frac{4F^2}{\pi^2} \sin^2\left(\arccos\left(\sqrt{1 - \frac{L}{R}}\right)\right)\right]^{1/2}}. \quad (16)$$

III. EXPERIMENT

The implementation of a high-precision static alignment scheme based on first-order modes (TEM_{10}, TEM_{01}) firstly requires overcoming the suppression of HGS modes by a high-finesse cavity. A series of approaches such as optical power amplifiers were adopted in the experiments to improve

the detection efficiency of the first-order mode. The following points should be highlighted for the experiments. (1) The purpose of this work is the development of a high-precision static alignment of the cavity HGS mode without measuring the ring-down absorption of the gas, and therefore no physical solid cavity was used. (2) The system in Figure 6 was mounted on the same vibration isolation stabilization platform. (3) A static high-precision alignment of the light source with the laser in the cavity was achieved by the alignment mirrors M1 and M2 controlled by the piezoelectric transducer (PZT). (4) All six-dimensional precision adjustment frames (APFP-XYZTθ) and CRD mounts (standard mirror mounts-902-0008) were centered in line with the centers of the optical elements. (5) Matching mirrors were designed. It is also necessary to simulate the beam waist radius of the two orthogonal planes in the whole optical path, and design the column lens so that the radii of the two orthogonal planes in the cavity are the same. The aim is to reduce the even-order HGS modes excited by astigmatism.

In order to improve the detection efficiency of the first-order mode, a polarization splitting method different from the conventional cavity ring-down experiments was used in the experiments. The s-polarized light was used as the reference beam to which a phase-modulated sideband was added in the experiment. The p-polarized light was also employed as the intracavity test beam to achieve a higher transmission coefficient. For achieving a higher finesse of the s-polarized light, the transmittance in P_1 and P_2 was smaller than that of p-polarized light. Therefore, the impedance matching condition will be broken and the injected power will be reduced. Entering the cavity is p-polarized light. The optical power amplifier is regarded as a booster optical amplifier (BOA1082P) that amplifies only p-polarized light.

The 2 MHZ single-mode laser emitted from the light source (DFB, EP1653-DM-B) firstly passes through the beam splitter and polarizing beam splitter. Then, the p-polarized light was passed through the matching mirror, M1, M2, and optical power amplifier into the CDR. The round-trip length of the triangular cavity was L=420 mm, and the reflectivity of P1 and P2 at 1653 nm was 99.997%. Additionally, the radius of curvature of P3 was 1 m, the reflectivity was 99.97%, and the angle between P1 and P2 was 88.542°. Therefore, the finesse of the cavity is about 26000 according to the finesse equation (17) of the triangular cavity. The S-polarized light emitted from the polarizing beam splitter was mixed with the cavity emitted light after the frequency sidebands after the phase modulator was added. The cavity length was also scanned by the PZT (PZT, P-841.10) controlled by the locking servo mechanism to lock the center frequency of the light source at the eigenfrequency of the fundamental mode in the cavity. For the ramp signal of the light source scan, a 15 Hz ring-down wave with a modulation range slightly larger than the FSR of the cavity was used, which was about 718 MHz. Thus, the resonance of the fundamental mode was ensured. It is important to note that the piezoelectric element attached to the end-mirror needs to be calibrated before the experiment to eliminate the hysteresis. After establishing the resonance of the fundamental mode, the

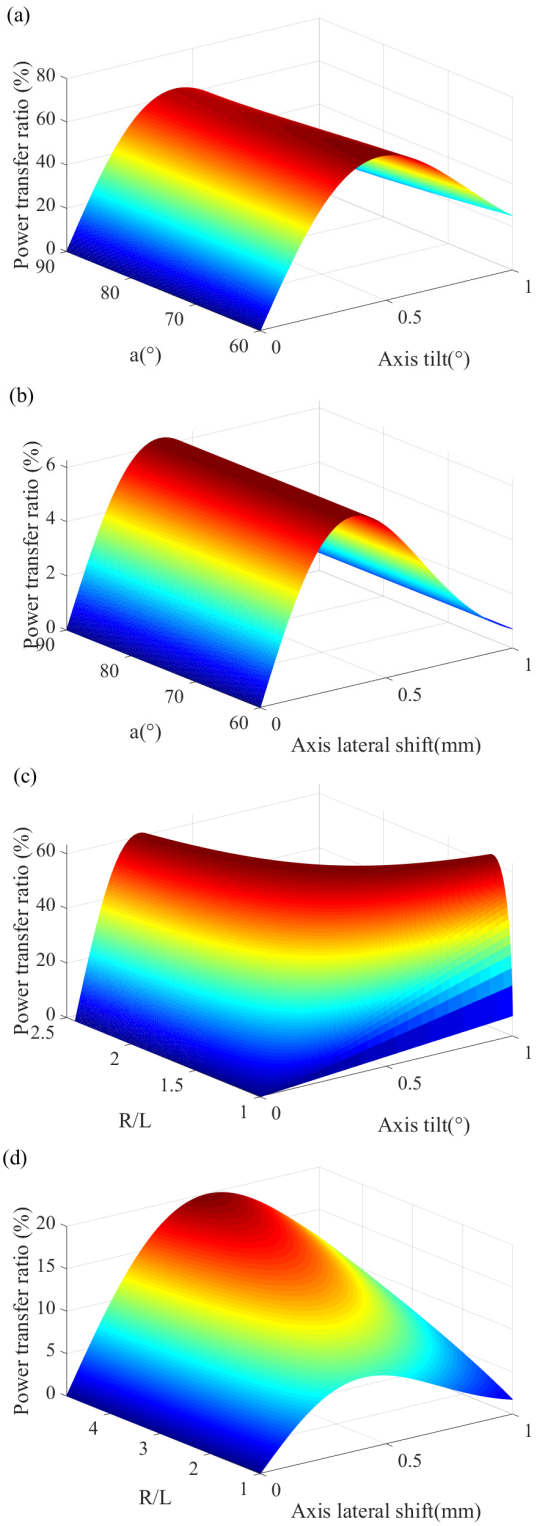

FIGURE 4. Power transfer in misalignment systems with first-order mode of Gaussian laser beams. The excitation intensity of the first-order mode varies with (a) α_x; and (b) ε_x at end-mirror radius R=1000, L=420 mm and varying angle α of the P_1P_2 clamp angle. The excitation intensity of the first-order mode varies with (c) α_x and (d) ε_x when the angle a = 88.56°, L = 420 mm, by varying R/L.

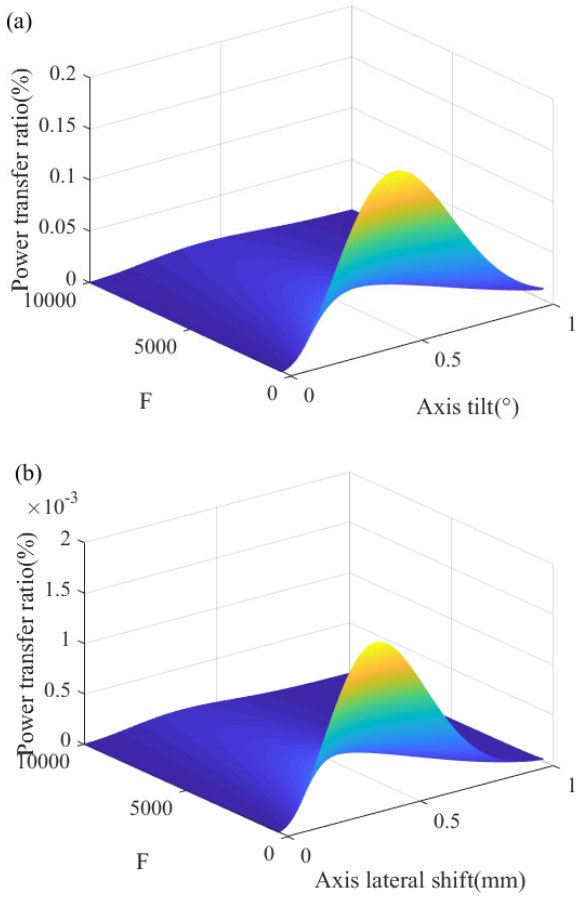

FIGURE 5. Distribution of the transmission intensity of the first-order mode as a function of (a) α_x and (b) ε_x when the finesse of the triangular CDR varies.

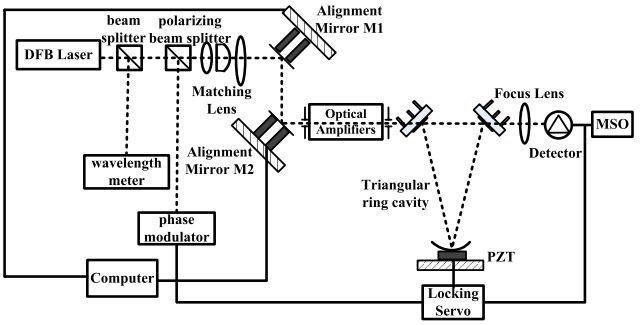

FIGURE 6. Structure diagram of triangular cavity static alignment experiment.

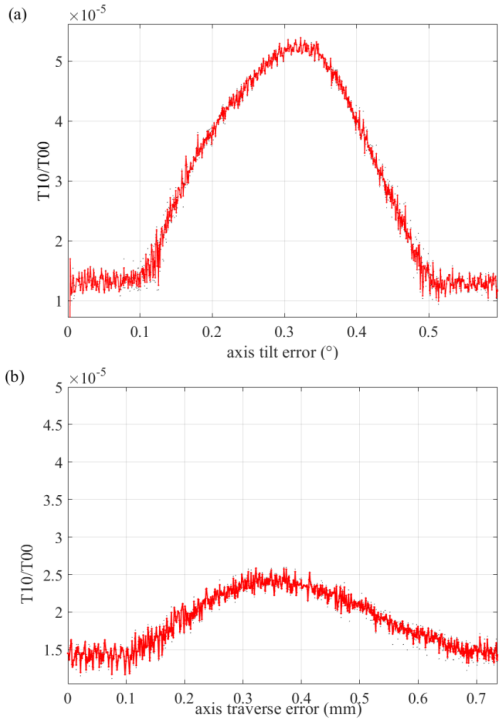

FIGURE 7. Variation of the first-order mode (TEM_{10}) power transfer ratio after the introduction of (a) α_x and (b) ε_x in the meridional plane.

frequency was swept by the control source of the wavelength meter (WaveCapture®FBGA-s). The sweep range is given by equation (14). The sweep was performed in the same way as the fundamental mode resonance was established. The light emitted from the CDR was focused on the detector through a large diameter short focal length lens. The optical signal was detected by using an InGaAs Switchable Gain Detector (thorlab PDA10CS2) and the output is fed to a digital oscilloscope (MSO, MSO6104A).

The introduction of misalignment error in the experiment was achieved by PZT controlling the alignment mirror M1 with M2. The tilt error was realized by the tilt of M2, and the axial shift error was realized by the simultaneous tilt of M1 and M2. To investigate the relationship between the misalignment error and the first-order mode excitation intensity, it is first necessary to control M1 and M2 to scan within the error range of 1° and 1.4 mm, and then detect the excitation value of the first-order mode. During the data analysis of misalignment errors, in order to eliminate repeatable residuals caused by oscilloscope channel crosstalk, multiple measurements need to be averaged to reduce the error. When the average number of times exceeds 64, the overall noise cannot be reduced further. Each error value corresponds to the average of 64 times the first-order mode excitation intensity.

Figure 7 shows the TEM_{10} excitation in the meridional plane. As can be observed, the TEM_{01} in the sagittal plane exhibits an excitation trend consistent with that of TEM_{10} in the experiment. In addition, the excitation intensity of the first-order mode in the experiment revealed a slower excitation enhancement and faster excitation weakening compared to the theoretical value in Eq. (16). This effect can be explained due to the gradual decrease of the light energy entering the detection system with the increase of the misalignment error.

The experiment also verified the independence of the first-order modes in two orthogonal planes, whereas the frequency separation property of the triangular cavity provided a theoretical basis for obtaining the error information of the two planes independently. The trend of the excitation of the

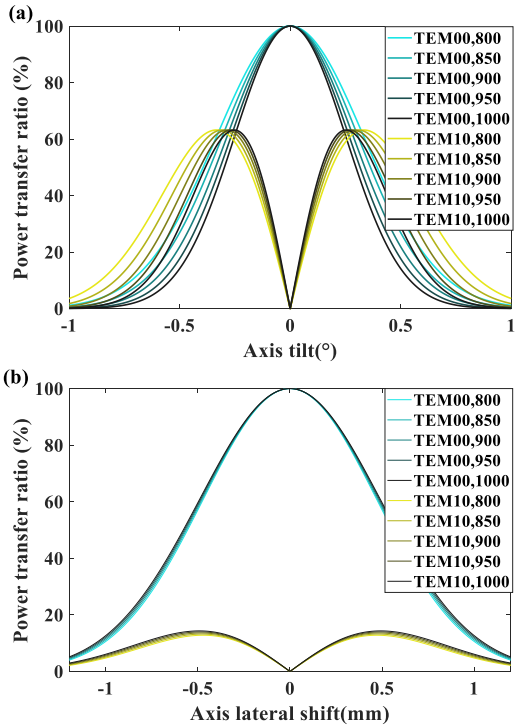

FIGURE 8. The first-order mode power transfer ratio follows a non-monotonic pattern as the misalignment increases, while the fundamental mode power transfer ratio is decreased monotonically. 800-1000 indicates different radii of curvature for P3.

first-order mode does not correspond to the trend of a specific amount of misalignment. A perfect static alignment scheme needs more information support.

IV. FURTHER DISCUSSION

Although the correlation between the first-order mode and the misalignment error was verified experimentally, it was limited by the following two points. More specifically, the excitation of the first-order mode was limited by noise and cannot respond when the error is too large ($\alpha_v > 0.5°$ and $\varepsilon_v > 0.7$ mm) and too small ($\alpha_v < 0.1°$ and $\varepsilon_v < 0.1$ mm). Another limitation of this scheme is the inability to determine the alignment mirror adjustment direction from the trend of the first-order mode. When the excitation of the first-order mode is detected to be weakened, the misalignment error at this time may correspond to both increasing and decreasing cases. It is thus obvious that the calibration direction cannot be obtained directly from the first-order mode information.

A complete mounting scheme requires the acquisition of more mode information. The excitation of the fundamental mode has been analyzed in detail in the study of Song [23]. The excitation of the fundamental mode showed monotonic weakening as the error was increased, which exactly compensates for the shortcoming of the first-order mode. The relationship between the fundamental mode and the misalignment error can be found in equation (18).

The frequency separation characteristics of the first-order mode of the triangular cavity and the monotonicity of the fundamental mode provide the conditions for achieving a high-precision static alignment of the triangular cavity. In order to achieve the alignment in the x-z plane during the alignment, it is necessary to obtain the fundamental mode and TEM_{10} information in the same error case successively. For the alignment of the x-z plane, it is necessary to read the fundamental mode and the TEM_{10} excitation of the two error points separately, where the TEM_{10} determines the plane information and the fundamental mode determines the adjustment direction. The sagittal plane was aligned in the same way as the meridional plane, by using the information from TEM_{01} and the base model.

V. CONCLUSION

In this work, the eigenfrequency separation characteristics of the same-order HGS mode specific to the triangular cavity were systematically analyzed based on the Hermite-Gaussian theory. The excitation characteristics were derived for different cavity structures with the first-order mode as an example. The sensitivity equation and the transmission characteristics of the HGS mode were studied for a high-finesse cavity. In the experiment, the transmission suppression of the first-order mode by the high finesse triangular cavity was overcome, and a static alignment scheme based on the eigenfrequency separation property of the first-order mode was designed. Finally, the fundamental mode information was added to compensate for the non-monotonicity drawback of the first-order mode. The theory and method of the static alignment stage of high finesse triangular CDR that was proposed in this work, verifies the feasibility of the HGS mode information to achieve accurate alignment, while a new improved idea for CRDS to achieve an enhanced theoretical sensitivity was also provided.

REFERENCES

[1] G. Berden, R. Peeters, and G. Meijer, "Cavity ring-down spectroscopy: Experimental schemes and applications," *Int. Rev. Phys. Chem.*, vol. 19, no. 4, pp. 565–607, Nov. 2010.

[2] G. N. Rao and A. Karpf, "High sensitivity detection of NO_2 employing cavity ringdown spectroscopy and an external cavity continuously tunable quantum cascade laser," *Appl. Opt.*, vol. 49, no. 26, pp. 4906–4914, Sep. 2010.

[3] G. Genoud, M. Vainio, H. Phillips, J. Dean, and M. Merimaa, "Radiocarbon dioxide detection based on cavity ring-down spectroscopy and a quantum cascade laser," *Opt. Lett.*, vol. 40, no. 7, pp. 1342–1345, Apr. 2015.

[4] A. Bicer, J. Bounds, F. Zhu, A. A. Kolomenskii, S. Tzortzakis, and H. A. Schuessler, "Cavity ring-down spectroscopy for the isotope ratio measurement of methane in ambient air with DFB diode laser near 1.65 μm," in *Proc. Conf. Lasers Electro-Opt. Eur. Eur. Quantum Electron. Conf. (CLEO/Eur.-EQEC)*, Jun. 2017, p. 1.

[5] C. E. Miller, L. R. Brown, R. A. Toth, D. C. Benner, and V. M. Devi, "Spectroscopic challenges for high accuracy retrievals of atmospheric CO_2 and the orbiting carbon observatory (OCO) experiment," *Comp. Rendus Phys.*, vol. 6, no. 8, pp. 876–887, Oct. 2005.

[6] D. R. Thompson, D. C. Benner, L. R. Brown, D. Crisp, V. Malathy Devi, Y. Jiang, V. Natraj, F. Oyafuso, K. Sung, D. Wunch, R. Castaño, and C. E. Miller, "Atmospheric validation of high accuracy CO_2 absorption coefficients for the OCO-2 mission," *J. Quant. Spectrosc. Radiat. Transf.*, vol. 113, no. 17, pp. 2265–2276, Nov. 2012.

[7] W. Chen, K. Roslund, C. L. Fogarty, P. J. Pussinen, L. Halonen, P.-H. Groop, M. Metsälä, and M. Lehto, "Detection of hydrogen cyanide from oral anaerobes by cavity ring down spectroscopy," *Sci. Rep.*, vol. 6, no. 1, Mar. 2016, Art. no. 22577.

[8] C. Wang, A. Mbi, and M. Shepherd, "A study on breath acetone in diabetic patients using a cavity ringdown breath analyzer: Exploring correlations of breath acetone with blood glucose and glycohemoglobin A1C," *IEEE Sensors J.*, vol. 10, no. 1, pp. 54–63, Jan. 2010.

[9] P. Jacquet, A. Pailloux, G. Aoust, J.-P. Jeannot, and D. Doizi, "Cavity ring-down spectroscopy for gaseous fission products trace measurements in sodium fast reactors," in *Proc. 3rd Int. Conf. Advancements Nucl. Instrum., Meas. Methods Their Appl. (ANIMMA)*, Jun. 2013, pp. 1–5.

[10] T. K. Boyson, D. R. Rittman, T. G. Spence, K. P. Kirkbride, D. S. Moore, and C. C. Harb, "Rapid, wideband cavity ringdown spectroscopy for the detection of explosives," in *Proc. CLEO*, Jun. 2014, pp. 1–2.

[11] A. Maity, S. Maithani, and M. Pradhan, "Cavity ring-down spectroscopy: Recent technological advancements, techniques, and applications," *Anal. Chem.*, vol. 93, no. 1, pp. 388–416, Jan. 2021.

[12] L. Gianfrani, "Linking the thermodynamic temperature to an optical frequency: Recent advances in Doppler broadening thermometry," *Phil. Trans. Roy. Soc. A: Math., Phys. Eng. Sci.*, vol. 374, no. 2064, Mar. 2016, Art. no. 20150047.

[13] D. A. Long, M. Okumura, C. E. Miller, and J. T. Hodges, "Frequency-stabilized cavity ring-down spectroscopy measurements of carbon dioxide isotopic ratios," *Appl. Phys. B, Lasers Opt.*, vol. 105, no. 2, pp. 471–477, Nov. 2011.

[14] B. A. Paldus, "Cavity-locked ring-down spectroscopy," *J. Appl. Phys.*, vol. 83, no. 8, pp. 3991–3997, 1998.

[15] M. D. Ghauri, S. Z. Hussain, U. Ullah, R. M. A. Ayaz, R. S. Z. Saleem, A. Kiraz, and M. I. Cheema, "Detection of aflatoxin m1 by fiber cavity attenuated phase shift spectroscopy," *Opt. Exp.*, vol. 29, no. 3, pp. 3873–3881, 2021.

[16] S. Wojtewicz, "Response of an optical cavity to phase-controlled incomplete power switching of nearly resonant incident light," *Opt. Exp.*, vol. 26, no. 5, pp. 5644–5654, Mar. 2018.

[17] R. W. P. Drever, J. L. Hall, and F. V. Kowalski, "Laser phase and frequency stabilization using an optical resonator," *Appl. Phys. B, Lasers Opt.*, vol. 31, no. 2, pp. 97–105, 1983.

[18] E. D. Black, "An introduction to Pound–Drever–Hall laser frequency stabilization," *Amer. J. Phys.*, vol. 69, no. 1, pp. 79–87, Jan. 2001.

[19] S. Solimeno and A. Cutolo, "Coupling coefficients of mismatched and misaligned Gauss–Hermite and Gauss–Laguerre beams," *Opt. Lett.*, vol. 11, no. 3, pp. 141–143, Mar. 1986.

[20] D. Z. Anderson, "Alignment of resonant optical cavities," *Appl. Opt.*, vol. 23, no. 17, pp. 2944–2949, Sep. 1984.

[21] N. M. Sampas and D. Z. Anderson, "Stabilization of laser beam alignment to an optical resonator by heterodyne detection of off-axis modes," *Appl. Opt.*, vol. 29, no. 3, pp. 394–403, Jan. 1990.

[22] M. R. Sayeh, H. R. Bilger, and T. Habib, "Optical resonator with an external source: excitation of the Hermite-Gaussian modes," *Appl. Opt.*, vol. 24, no. 22, pp. 3756–3761, Nov. 1985.

[23] S. Song, C. Hu, and C. Yan, "Optical axis maladjustment sensitivity in a triangular ring resonator," *Appl. Opt.*, vol. 58, no. 1, pp. 29–36, Jan. 2019.

[24] Y. Ren, C. Yan, C. Wu, S. Song, and J. Yuan, "Resonant frequency separation characteristics of the same-order Hermite-Gaussian mode in the astigmatic triangular cavity of a cavity ring-down cpectroscope," *IEEE Access*, vol. 10, pp. 53703–53712, 2022.

[25] H. Huang and K. K. Lehmann, "Sensitivity limits of continuous wave cavity ring-down spectroscopy," *J. Phys. Chem. A*, vol. 117, no. 50, pp. 13399–13411, Dec. 2013.

[26] A. Karpf, Y. Qiao, and G. N. Rao, "Ultrasensitive, real-time trace gas detection using a high-power, multimode diode laser and cavity ringdown spectroscopy," *Appl. Opt.*, vol. 55, no. 16, pp. 4497–4504, Jun. 2016.

[27] L. E. McHale, A. Hecobian, and A. P. Yalin, "Open-path cavity ring-down spectroscopy for trace gas measurements in ambient air," *Opt. Exp.*, vol. 24, no. 5, pp. 5523–5535, Mar. 2016.

[28] J. W. Hahn, Y. S. Yoo, J. Y. Lee, J. W. Kim, and H. W. Lee, "Cavity ringdown spectroscopy with a continuous-wave laser: calculation of coupling efficiency and a new spectrometer design," *Appl. Opt.*, vol. 38, no. 9, pp. 1859–1866, Mar. 1999.

[29] K. W. Busch and M. A. Busch, "Introduction to cavity-ringdown spectroscopy," in *Proc. Cavity-Ringdown Spectrosc., ACS Symp. Ser.*, 1999, pp. 7–19.

[30] D. Romanini and K. K. Lehmann, "Ring-down cavity absorption spectroscopy of the very weak HCN overtone bands with six, seven, and eight stretching quanta," *J. Chem. Phys.*, vol. 99, no. 9, pp. 6287–6301, Nov. 1993.

[31] L. W. Casperson, "Synthesis of Gaussian beam optical systems," *Appl. Opt.*, vol. 20, no. 13, pp. 2243–2249, 1981.

[32] C. Mathis, C. Taggiasco, L. Bertarelli, I. Boscolo, and J. R. Tredicce, "Resonances and instabilities in a bidirectional ring laser," *Phys. D, Nonlinear Phenomena*, vol. 96, nos. 1–4, pp. 242–250, Sep. 1996.

[33] A. E. Siegman, "Orthogonality properties of optical resonator eigenmodes," *Opt. Commun.*, vol. 31, no. 3, pp. 369–373, Dec. 1979.

YIJIE REN was born in Changzhi, Shanxi, China, in 1994. He received the B.S. degree in measurement and control technology and instrument from the Changchun University of Science and Technology, China, in 2018. He is currently pursuing the Ph.D. degree in optical engineering with the Changchun Institute of Optics, Fine Mechanics and Physics, Chinese Academy of Sciences, Changchun, China. His current research interests include cavity ring-down spectroscopy and trace gas detection.

CHANGXIANG YAN was born in Honghu, Hubei, China, in 1973. He received the M.S. degree in engineering from Zhejiang University, Zhejiang, China, in 1998, and the Ph.D. degree from the Changchun Institute of Optics, Fine Mechanics and Physics, Chinese Academy of Sciences, Changchun, China in 2001.

Since 2010, he has been the Director of the Space Optics Laboratory, Changchun Institute of Optics, Fine Mechanics and Physics, Chinese Academy of Sciences. His research interests include opto-mechatronics technology for space optical remote sensing instruments, multispectral and hyperspectral spatial remote sensing imaging, cavity ring-down spectroscopy, polarization detection, and space surveillance.

CONGJUN WU was born in Ankang, Xian, China, in 1986. He received the Ph.D. degree from the Changchun Institute of Optics, Fine Mechanics and Physics, Chinese Academy of Sciences, Changchun, China, in 2014. His current research interests include optical design and optical system image quality research.

XIAOQUAN BAI was born in Changchun, Jilin, China, in 1993. He received the B.S. degree in opto-electronic information science and engineering from the Changchun University of Science and Technology, China, in 2017, and the Ph.D. degree from the Changchun Institute of Optics, Fine Mechanics and Physics, Chinese Academy of Sciences, Changchun, China, in 2022. His current research interest includes on-orbit aberration compensation strategies for space telescopes

ZHIWEI CHEN was born in Honghu, Hubei, China, in 1998. He received the B.S. degree in optical information science and technology from Yangtze University, China, in 2019. He is currently pursuing the Ph.D. degree in optical engineering with the Changchun Institute of Optics, Fine Mechanics and Physics, Chinese Academy of Sciences, Changchun, China. His current research interest includes telescope stability analysis in space gravitational wave detection.